Conformational analysis of 2-(carboxycyclopropyl)glycine agonists of glutamate receptors in aqueous solution using a combination of NMR and molecular modelling experiments and charge calculations

Nathalie Evrard-Todeschi,[a] Josyane Gharbi-Benarous,[a,b] Aliette Cossé-Barbi,[c] Gérard Thirot[c] and Jean-Pierre Girault*,[a]

[a] *Laboratoire de Chimie et Biochimie Pharmacologiques et Toxicologiques (URA 400 CNRS), Université René Descartes, 45 rue des Saint-Péres, 75270 Paris Cedex 06, France*
[b] *UFR Chimie Université Paris 7, Denis Diderot, 2 Place Jussieu, F-75251 Paris Cedex 05, France*
[c] *Institut de Topologie et Dynamique des Systemes (URA 34 CNRS), Université Paris 7, Denis Diderot, 1 Rue Guy de La Brosse, F-75005 Paris Cedex 05, France*

Two classes of glutamate receptors [metabotropic (group-II) and ionotropic (NMDA) subclasses] are characterized by the binding of α-(carboxycyclopropyl)glycine (CCG) isomers, (2*S*,3*S*,4*S*)-CCG (L-CCG-I) and (2*S*,3*R*,4*S*)-CCG (L-CCG-IV) which contain an embedded L-glutamate moiety in a partially restricted conformation [relative to the C(3)–C(4) bond]. The spatial orientation of the perceived functional groups have been elucidated by a conformational analysis in aqueous solution of L-CCG-I and L-CCG-IV using a combination of NMR experimental results, theoretical simulation of NMR spectra, mechanics and dynamics calculations. It was of interest to compare the charge distributions resulting from a number of quantum calculations on the cyclopropane ring. One important conclusion of the study is that the best theoretical model is the MD in solvent. This study shows clearly the preferred '*t*-A' and 'g^+-B' conformations of the C(3) aminocarboxymethyl side chain for L-CCG-I and L-CCG-IV, respectively. Weak pH-dependent effects on the structure of the principal L-CCG-I and L-CCG-IV conformers have been established in aqueous solution. The conformations may be grouped by the two backbone torsion angles, χ_1 [α-CO_2^-–C(2)–C(3)–C(4)] and χ_2 [$^+$NC(2)–C(3)–C(4)–γ-CO_2^-] and by the two characteristic distances between the potentially active functional groups, α-N^+–γ-CO_2^- (d_1) and α-CO_2^-–γ-CO_2^- (d_2). The conformational preferences in solution of L-CCG-I and L-CCG-IV are discussed in the light of the physical features known for specific metabotropic (ACPD) and specific ionotropic (NMDA) agonists, respectively.

Introduction

Excitatory amino acid receptors are now generally accepted as the main transmitter receptors in the mammalian central nervous system, with glutamate[1–3] in particular playing an important role in synaptic plasticity phenomena involved in brain development, learning and memory. Dysfunction of these systems leads to various neurological disorders such as epilepsy, plasticity and Huntington's disease.

Glutamate receptors have been classified into two types: the ionotropic and metabotropic (mGluRs) receptors.[2,3] The former are further subdivided into three subtypes[4–6] termed *N*-methyl-D-aspartic acid (NMDA), aminohydroxy-5-methylisoxazol-4-yl propionate (AMPA) and Kainic acid [KA, 2-carboxy-4-(1-methylethenyl)pyrrolidine-3-acetic acid]. The mGluRs[7,8] are coupled to G-proteins and to date, eight mGluRs[9,10] have been characterized and classified into three groups: group-I (mGluR1 and mGluR5) coupled to phospholipase C and activated by *trans*-1-aminocyclopentane-1,3-dicarboxylate (1*S*,3*R*-*trans*-ACPD) and quisqualate (QUIS); group-II (mGluR2 and mGluR3) negatively coupled to adenylyl cyclase and activated by (1*S*,3*R*)-*trans*-ACPD and α-(carboxycyclopropyl)glycine (2*S*,3*S*,4*S*-**L-CCG-I**); group-III (all the other mGluRs) also negatively coupled to adenylyl cyclase but selectively activated by L-AP4.[10]

As an acyclic molecule, glutamate can adopt nine staggered conformers resulting from rotation about C(2)–C(3) and C(3)–C(4) bonds (Fig. 1) and is therefore capable of fitting the different types of receptors.[2] Any bound form of L-glutamate would most likely resemble one of the solution conformers, since binding of conformations other than local minima (*e.g.* eclipsed conformers) would automatically incur an energy penalty.[11]

One method used for determining structure–activity relationships is the production of rigid analogues of glutamic acid. The introduction of conformationally restricted analogues of natural amino acids into substrates or inhibitors has proved helpful for studies of the geometry of binding sites.[12] Conformationally restricted glutamate analogues such as (1*R*,3*R*)-*cis*-ACPD and (2*S*,3*R*,4*S*)-**L-CCG-IV** have been identified as potent agonists of the ionotropic NMDA receptor while (1*S*,3*R*)-*trans*-ACPD and (2*S*,3*S*,4*S*)-**L-CCG-I** activated the metabotropic mGluR2 receptor.[13,14] Indeed, selective binding of conformationally restricted analogues implies that glutamate may bind to each receptor in a distinct conformation.

Glutamic acid analogues containing a cyclopentane ring (ACPD isomers) have been already submitted to conformational analysis.[15,16] Cyclopentane (ACPD) isomers representing unstrained cyclic analogues resemble some staggered conformations of glutamate quite closely with respect to the relative positions of the polar functional groups. On the other hand, cyclopropyl (CCGs) analogues might resemble intermediate rotamers because of bond angle deformation due to ring strain and to differences in preferred torsional angles between cyclic and acyclic (glutamate) hydrocarbon chains.

In this paper, we describe a conformational analysis by ^{1}H and ^{13}C NMR spectroscopy and molecular modelling of **L-CCG-I** and **L-CCG-IV** isomers [Fig. 2(*a*)]. Here, the rotation about the C(3)–C(4) bond (χ_2 dihedral angle) is frozen, and so the nine conformations of glutamate (Fig. 1) are restricted to only three rotamers (Figs. 3 and 4) resulting from rotation about the C(2)–C(3) bond (χ_1 dihedral angle). Thus, this study

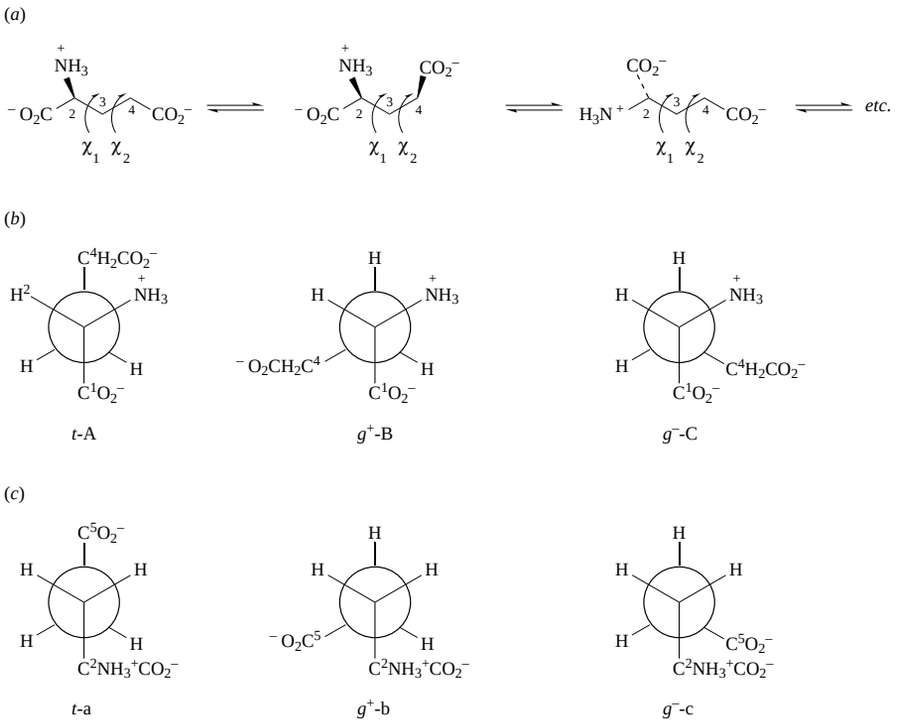

Fig. 1 (*a*) Conformers of L-glutamate; (*b*) newman projections for the three χ_1 [C(2)–C(3)] rotamers '*t*-A, g^+-B, g^--C' and (*c*) the three χ_2 [C(3)–C(4)] '*t*-a, g^+-b, g^--c' rotamers (*t*, *anti* and *g*, *gauche*)

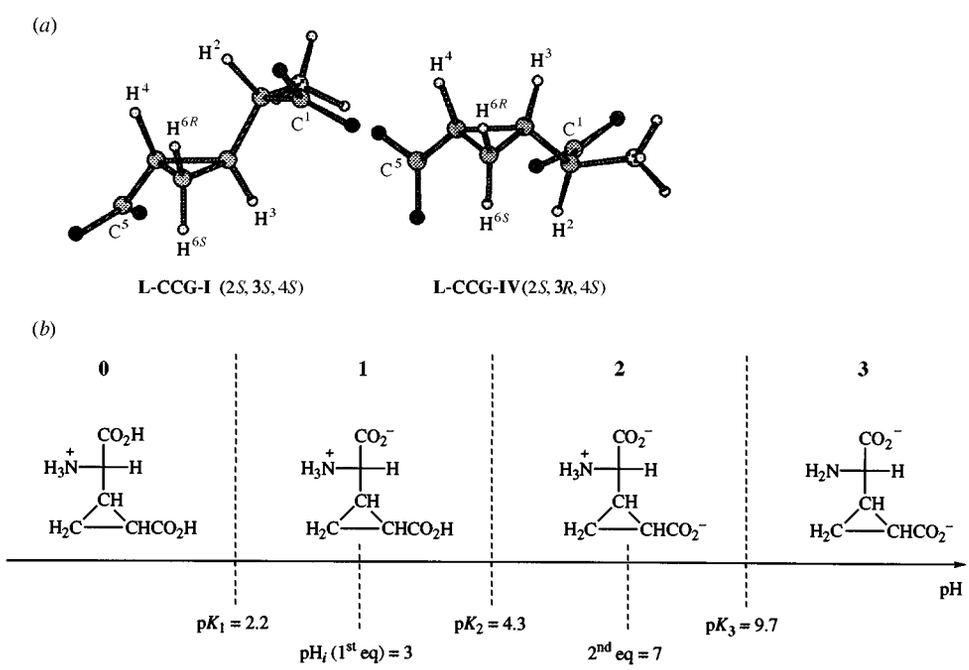

Fig. 2 (*a*) Structure of **L-CCG** in aqueous solution at pH 7 (isomers α-*S* represented); (*b*) predominant forms of **L-CCG** isomer in the different pH zones (from 0 to 3)

might allow us to shed light on the resulting conformation of **L-CCG** analogues in aqueous solution.

NMR experiments and computational investigation were undertaken in water in order to elucidate the conformational characteristics in a biological-type environment.

A conformational search on the molecules whose ionized functional groups are γ-CO_2^-, α-CO_2^- and α-NH_3^+ was performed by NMR spectroscopy (study at physiological pH) and molecular dynamics (MD). However, the receptor may be an acceptor or a donor of protons. Hence, a number of structural features defined by the relative positions of the charged heteroatoms and the position of the hydrocarbon backbone can affect binding affinities. Thus, we have extended the NMR studies in water at different pH values [Fig. 2(*b*)], so as not to neglect protonation effects which will induce particular conformations. MD studies were performed on corresponding protonated or non-protonated species.

Making use of the relevant structures generated by MD, the experiments provide useful information on the conformational behaviour of aqueous (carboxycyclopropyl)glycine derivatives using experimental values for the vicinal homo- and heteronuclear coupling constants, pH dependence of coupling constants and chemical shift data. For those compounds bearing a three-membered ring, particular problems arise due to ring strain or, in other words, to the deviation from the classical sp^3 hybridization. Atypical atomic charges and particular effects on

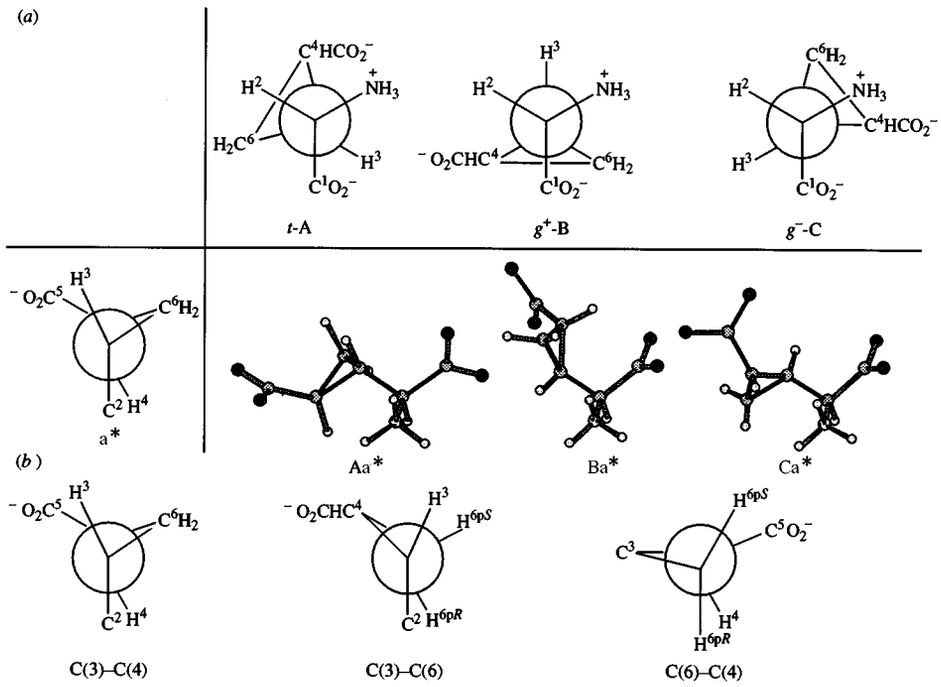

Fig. 3 Newman projections of **L-CCG-I** for (*a*) the three χ_1 '*t*-A, g^+-B, g^--C' [C(2)–C(3)] rotamers and the eclipsed χ_2 '*e*-a*' [C(3)–C(4)] rotamer, (*b*) views down the [C(3)–C(4)], [C(3)–C(6)] and [C(6)–C(4)] bonds, respectively

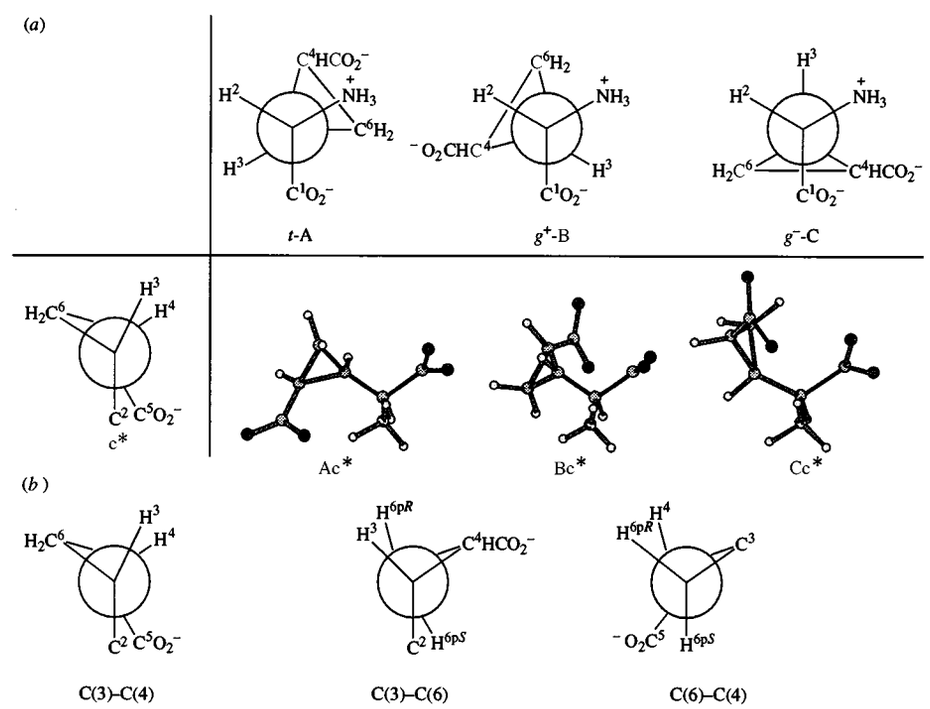

Fig. 4 Newman projections of **L-CCG-IV** for (*a*) the three χ_1 '*t*-A, g^+-B, g^--C' [C(2)–C(3)] rotamers and the eclipsed χ_2 '*e*-c*' [C(3)–C(4)] rotamer, (*b*) views down the [C(3)–C(4)], [C(3)–C(6)] and [C(6)–C(4)] bonds, respectively

some coupling constants are expected. These points will be examined with caution. As a result, this extensive conformational study of (carboxycyclopropyl)glycine (CCGs) shall provide the basis for further molecular modelling and NMR studies of CCGs analogues or aminocyclopropanecarboxylic acid (ACC) derivatives. Previous studies of CCGs derivatives[17,18] have postulated an hypothesis about the conformational requirement of metabotropic and ionotropic (NMDA) glutamate receptors that it was interesting to strengthen as these studies were based on an experimental homonuclear coupling constant value about C(2)–C(3) (χ_1 dihedral angle) and on calculations for which solvent and charges have not been considered.

Results and discussion

A conformational search was performed on the zwitterionic molecules at neutral pH with ionized functional groups γ-CO_2^-, α-CO_2^- and α-NH_3^+. However, as three acidity functions are present in these compounds (pK_a = 2.2, 4.3 and 9.7), the charges of groups and their protonation depend on the pH of solution; three predominant forms [Fig. 2(*b*)] must be taken into account for the study in aqueous solution from pH range **1** (pH ≤ 3) to **3** (pH ≥ 10). The preferred conformation may depend on these charges because of the electrostatic interactions or hydrogen bonding implied. At isoelectric pH (pH_i = 3), the γ-carboxylate group is protonated and can provide a distal carboxylic acid

Table 1 Homonuclear (^{1}H,^{1}H) and heteronuclear (^{13}C,^{1}H) coupling constants in D_2O (error, 0.3 Hz) corresponding to the torsion angle in the cyclopropane used for the assignment of diastereotopic methylene protons at C(6) and for the adjustment of Karplus-type equations required for the conformational analysis of **L-CCG-I** and **L-CCG-IV**

	L-CCG-I			**L-CCG-IV**		
Proton	Theoretical torsion angles/°	Theoretical ^3J/Hz	NMR ^3J/Hz	Theoretical torsion angles/°	Theoretical ^3J/Hz	NMR ^3J/Hz
3, 4	−150.1	6.9	4.2	−0.5	8.2	9.0
3, 6′	3.2	8.2	8.8	−1.6	8.2	8.8
3, 6″	150.6	7.0	5.8	153.7	7.4	6.8
4, 6′	150.0	6.9	5.3	4.7	8.2	8.5
4, 6″	4.3	8.2	8.7	145.8	6.3	5.5
H3, C5	−9.8	5.4	3.7	147.1	5.0	2.9
H4, C2	−3.8	5.6	4.4	−147.2	5.0	2.3
H6′, C2	−146.4	4.8	3.9	139.7	4.3	2.2
H6′, C5	7.4	5.5	4.7	−134.8	3.8	2.5
H6″, C2	4.9	5.6	5.3	−12.4	5.4	5.1
H6″, C5	−140.0	4.3	2.9	6.3	5.5	5.0
Assignment						
6′-H	*S*			*R*		
6″-H	*R*			*S*		
NOEs	[4-H]6″-H [3-H]6′-H [2-H]6″-H			[4-H]6′-H [3-H]6′-H		

[a] The coupling constants $^3J_{HH}$ and $^3J_{HC}$ were calculated by using Karplus-type equations: in the homonuclear case, $^3J_{HH} = 4.5 \cos 2\varphi - 0.5 \cos \varphi + 4.22$[37] and in the heteronuclear case, $^3J_{HC} = 5.7 \cos^2 \varphi - 0.6 \cos \varphi + 0.5$.[36]

which possesses a potential proton donor hydroxy group. At the opposite extreme, a pH = 10, the amino group carries no formal charge.

Details of NMR spectra and methods of spectral analysis are reported in this paper. Energy calculations for these substituted systems are then described which support the existence of a three-well energy profile for the rotation of the C–C single bond between the cyclopropyl ring and the amino acid group. Molecular dynamic (MD) calculations deal with the energy and geometry of individual conformations, whereas NMR data are averaged over different conformations; this study serves to correlate the two methods. The modelling procedure used to generate the approximate ratios of low-energy conformers will also specify the structures representative of very hindered intermediates.

NMR spectroscopy

Large deviations in bond angles from the normal values are found in cyclopropane and other molecules containing three-membered rings. Rules and regularities relative to chemical shifts and coupling constants tend to fail in these cyclic compounds because their conformations are more rigidly defined and anisotropic shielding effects are more prominent. A modified Karplus equation for the dependence of the vicinal coupling constants ^3J on the torsion angle will be used.

Due to the dependence of vicinal coupling constants on the χ_1 torsion angle, NMR spectroscopy has increased our knowledge about rotational isomers in cyclopropane systems. The conformation of substituted three-membered rings has been investigated in several studies.[19–23] Rotation about the C(2)–C(3) bond is characterized by a three-well energy profile in which the *trans* H(2)–H(3) form is at the minimum and two *gauche* forms are at higher energy [Figs. 3(*a*) and 4(*a*)].

2-(Carboxycyclopropyl)glycines (CCGs) are conformationally restricted glutamate analogues in which the cyclopropyl ring partially fixes the glutamate chain [C(3)–C(4)]. Concerning the rotamer around the α-amino acid moiety of CCGs, it can be assumed that the C(2)–C(3) bond can rotate freely [Figs. 3(*a*) and 4(*a*)]. The C(1)–C(2)–C(3)–C(4) system allows the possibility of *trans* and *gauche* forms and we obtain three staggered χ_1 (*t*-A, g^+-B and g^--C) rotamers resulting from rotation about the χ_1 [α-CO_2^-–C(2)–C(3)–C(4)] torsion angle.

For **L-CCG**, rotation around the C(3)–C(4) bond is totally restricted and the staggered χ_2 (*t*-a, g^+-b and g^--c) rotamers of glutamate (Fig. 1) are prevented by the three-membered ring. The χ_2 [C(2)–C(3)–C(4)–γ-CO_2^-] torsion angle adopts eclipsed forms characterized by an intermediate angle value, *e*-a* ($\chi_2 = 150$–$120°$) in **L-CCG-I** between *trans t*-a ($\chi_2 = 180°$) and *gauche* g^+-b ($\chi_2 = 60°$) orientations [Fig. 3(*b*)] and *e*-c* ($\chi_2 = -20$–$10°$) in **L-CCG-IV** between two *gauche* g^--c ($\chi_2 = -60°$) and g^+-b ($\chi_2 = 60°$) orientations [Fig. 4(*b*)].

Assignments. For an unambiguous interpretation of the conformational NMR data, the complete assignment of the ^{1}H NMR and ^{13}C spectra was an absolute prerequisite. The study was carried out on an AMX 500 spectrometer on samples dissolved in deuterium oxide at three pH values: 3 (isoelectric), 7 (neutral) and 10 (basic).

The assignments of proton and carbon resonances are given in Table S1 of the supplementary material.† Carbon assignments were assigned almost completely from broad-band decoupled ^{13}C spectra and a DEPT 135 experiment. The carboxylate groups (α- and γ-CO_2^-) and the methylene groups (3-CH and 4-CH) were differentiated by a selective INEPT experiment[24–26] based on a selective excitation of the H(2) since they were ^{1}H, ^{13}C long-range coupled to H(2). Thus, it was possible to confirm assignments of the corresponding proton H(3) with lower frequency and H(4) with higher frequency from inverse heteronuclear COSY,[27] as they are simultaneously coupled to the carbons C(3) and C(4), respectively.

Assignment of diastereotopic protons.—The prefixes *R* and *S* were used to unambiguously designate the configuration of the prochiral centre. The assignment of the individual diastereotopic methylene protons was particularly difficult. Qualitative considerations are often used for diastereotopic assignment of methylene protons.[28]

The assignments were essentially obtained by analysing all the $^3J_{HH}$ and $^3J_{CH}$ coupling constants (Table 1) measured from H(6′) and H(6″). The most important coupling constants involve the C-atom of the amino acid group, C(2), and 5-

† Supplementary material is available (suppl. no. 57297, 6pp) from the British Library. For details of the Supplementary Publications Scheme, see 'Instructions for Authors', *J. Chem. Soc.*, *Perkin Trans. 2*, 1997, issue 1.

Table 2 Homonuclear (^{1}H,^{1}H) and heteronuclear (^{13}C,^{1}H) coupling constants in D_2O (error, 0.3 Hz) corresponding to the torsion angle χ_1 and used in the conformational analysis of **L-CCG-I** and **L-CCG-IV**

	L-CCG-I				**L-CCG-IV**			
		Theoretical torsion angles/° (^3J/Hz)[a,b]				Theoretical torsion angles/° (^3J/Hz)[a,b]		
Rotamer around χ_1	NMR (^3J/Hz)	A	B	C	NMR (^3J/Hz)	A	B	C
2, 3		−170.3	59.0	−57.5		−53.7	−177.8	45.0
	10.0	(12.1)	(3.4)	(3.7)[a]	8.0	(4.1)	(12.4)	(5.4)[a]
H2, C4		31.8	−82.1	156.2		89.2	−35.1	−168.6
	2.0	(3.3)	(0.5)	(4.6)[b]	2.3	(0.5)	(3.8)	(3.7)[b]
H2, C6		−38.1	−156.5	82.9		166.9	38.8	−92.6
	2.3	(2.9)	(4.6)	(0.3)[b]	2.0	(3.6)	(3.5)	(1.2)[b]
H3, C1		−60.2	179.7	57.8		59.3	−63.2	160.5
	2.3	(1.6)	(6.8)	(1.8)[a]	2.6	(1.7)	(1.4)	(6.0)[a]
NOEs	[2-H]4-H							
	[2-H]6″-H				[2-H]6″-H			
Populations of rotamers about χ_1								
		75	15	10		35	45	20

[a] The coupling constant values $^3J_{HH}$ and $^3J_{HC}$ were calculated by using Karplus-type equations: in the homonuclear case,[33] $^3J_{HH} = 9.5 \cos^2 \varphi - 1.4 \cos \varphi + 1.9$ and in the heteronuclear case,[36] $^3J_{HC} = 5.7 \cos^2 \varphi - 0.6 \cos \varphi + 0.5$. [b] The values of heteronuclear $^3J_{HC}$ in the three theoretical rotamers were calculated using $^3J_{HC} = 5.7 \cos^2 \varphi - 0.6 \cos \varphi + 0.5$;[37] these couplings imply that bonds in the cyclopropane ring were adjusted by the parameters mentioned hereafter: $^3J_t = {}^3J_{calc} \times 0.6$ and $^3J_g = {}^3J_{calc} \times 0.8$.

carboxylate groups, as their long-range couplings allow the assignment of the diastereotopic protons of the adjacent C(6) methylene group.[29–31]

The relation $^3J_{trans} < {}^3J_{cis}$ relative to homonuclear and heteronuclear coupling constants and specific to the three-membered ring, was also used to confirm the stereospecific assignment of the protons H(6).

Stereospecific assignments[30,31] were also obtained by the analysis of NOE effects from H(6′) and H(6″) protons. The position of H(6) protons relative to one face of the three-membered ring was deduced from NOE experiments involving H(6), H(2) and H(3) protons when they were located in the same face (Table 1 and Fig. S1 of the supplementary material). The measured distances between H(6), H(2) and H(3) protons in the three rotamers (A, B, C) from molecular modelling calculations were compared to those obtained by NMR spectroscopy (^{1}H NOESY experiment). These observations may be rationalized by the presence of a predominant 'A' χ_1 rotamer for **L-CCG-I** (Fig. 3) and the diastereotopic assignment of H(6) protons H(6′) and H(6″).

Coupling constants. Accurate homo- and hetero-nuclear coupling constants can serve to determine the population of χ_1 rotamers (Figs. 3 and 4) and ^3J values were used to establish the major solution state conformations of these compounds. The homonuclear and heteronuclear three-bond coupling constants were also necessary for the assignments of diastereotopic protons H(6).

The Karplus-type equation describes quite satisfactorily the dependence of the vicinal H,H (or H,C) coupling constant on the torsion angle for a large number of compounds. However, special circumstances exist in the case of the three-membered ring. Here the dihedral angle for *cis* is ~0° and for *trans* directions is ~150°. According to the Karplus curve, we could expect that $^3J_{trans} < {}^3J_{cis}$, and this is always found experimentally for a pair of *cis–trans* isomers of a substituted cyclopropane.

As the protons H(2), H(3), H(4), H(6′) and H(6″) constituted a highly coupled system, the *J*- and δ-values were calculated after the simulation of the NMR spectrum by the standard Bruker package PANIC (parameter adjustment in NMR by iterative calculation). The analysis of the five-spin system was refined by spectral simulation using the NMR II software. The spectra calculated from the *J*- and δ-values, reported in Tables 1 and 2, were in agreement with the experimental data. Homonuclear coupling constants in acidic and basic solution are summarized in Table S2. The ^3J values were less sensitive to pH for **L-CCG-I** than for **L-CCG-IV**. Thus, the population of χ_1 rotamers did not change appreciably for **L-CCG-I** as they did for **L-CCG-IV**.

Determination of heteronuclear long-range ^{13}C–^{1}H coupling constants by the selective 2D INEPT experiment[32] was especially helpful in ascertaining the relative position of the substituents (α-CO_2^-, γ-CO_2^-, cyclopropyl) with respect to the backbone. Heteronuclear (^{13}C, ^{1}H) coupling constants were difficult to measure in acidic and basic solution because of overlapping ^{1}H multiplets and problems encountered with T_2 relaxation. Thus, it was not possible to exactly evaluate the population of χ_1 rotamer at these pH values.

Karplus equations. In conformational studies by NMR, the three-membered ring is a special case among the amino acids. In the cyclopropane, the torsion angles are restricted, and the conformation about the bond is fixed. Indeed, if one makes the assumption that the ring exists in a single conformation it is possible to test Karplus-type equations.[33–36] A comparison between theory and experiment was made by using information from a variety of conformationally rigid angles encountered in the cyclopropyl ring of **L-CCG-I** and **L-CCG-IV**.

Ten $^3J_{HH}$ and twelve $^3J_{HC}$ coupling constants were measured (Table 1) on the cyclopropyl unit relative to the C(3)–C(4), C(3)–C(6) and C(6)–C(4) bonds [Figs. 3(*b*) and 4(*b*)] for both **L-CCG-I** and **L-CCG-IV** and they correspond to a single strongly favoured eclipsed χ_2 conformation *e*-a* (χ_2 = 150–120°) for **L-CCG-I** and *e*-c* (χ_2 = −20–10°) for **L-CCG-IV**. Since there are 10 experimental homonuclear and 12 experimental heteronuclear coupling constant values (Table 1), one will compare them to coupling constants calculated with different Karplus equations. For our purposes, the corresponding torsion angles were determined by molecular modelling (see below) and the conformation of the three-membered ring system was then specified by *cis* H,H dihedral angles which varied from 0.5 to 4.7° and *trans* values from 145.8 to 153.7° while *cis* H,C dihedral angles varied from 3.8 to 12.4° and *trans* values from 134.8 to 147.2°.

The ^{13}C–^{1}H couplings, in combination with the ^{1}H–^{1}H coupling constants, are useful to provide Karplus-type equations that are better defined for three-membered rings. The equations used in the homonuclear case[37] and in the heteronuclear case[36]

have given results with an adequate approximation when they were applied to the **L-CCG-I** and **L-CCG-IV** model systems (Table 1).

Experience has shown that in general $^3J_{H,H}$ values for $\varphi \sim 0°$ were about 0.3–0.8 Hz larger while for $\varphi \sim 150°$, $^3J_{H,H}$ were about 0.7–2.7 Hz lower than the calculated values, although the prediction that $^3J_{trans} > {}^3J_{cis}$ was confirmed. An electronegativity correction is necessary and simple: in the homonuclear case [eqns. (1) and (2)] and heteronuclear case [eqns. (3) and (4)].

$$^3J_{obs} = {}^3J_{calc\text{-}trans} \times 0.8 \quad (1)$$

$$^3J_{obs} = J_{calc\text{-}cis} \times 1.1 \quad (2)$$

$$^3J_{obs} = J_{calc\text{-}trans} \times 0.6 \quad (3)$$

$$^3J_{obs} = J_{calc\text{-}cis} \times 0.8 \quad (4)$$

The values of homo- and hetero-nuclear long-range $^3J_{HH}$ and $^3J_{HC}$ provided evidence for the identification of the major rotamers for **L-CCG-I** and for **L-CCG-IV**. The determination of structures in solution results from a quantitative comparison of experimental and theoretical (from MD simulations) coupling constants relative to the three *t*-A, g^+-B and g^--C rotamers. Theoretical couplings (J_g and J_t) over the single bond between the cyclopropane ring and the α-amino acid moiety ($^3J_{H2C4}$ and $^3J_{H2C6}$) were adjusted by the parameters mentioned above, for **L-CCG-I** and **L-CCG-IV** (Table 2). Thus, the experimental values of $^3J_{H2C4}$ and $^3J_{H2C6}$ coupling constants have confirmed the population of the three rotamers *t*-A, g^+-B and g^--C determined by the conformational analysis.

Conformational analysis. In solution, the backbone of these analogues was found to be relatively rigid and it would thus be expected that much stereochemical and conformational data could be deduced from the $^3J_{^1H,^1H}$ and $^3J_{^{13}C,^1H}$ coupling constants. Side-chain atoms are allowed to rotate freely around the χ_1 [C(2)–C(3)] dihedral angle. NMR parameters should therefore be interpreted in terms of contributions from the staggered conformations corresponding to χ_1 values 180, 60 and −60° (*t*-A, g^+-B, g^--C χ_1 rotamers). The population of χ_1 rotamers was determined from experimental $^3J_{HH}$ and $^3J_{HC}$ coupling constants. Thus, it was possible to interpret $^3J_{H2H3}$, $^3J_{H2C4}$, $^3J_{H2C6}$ and $^3J_{H3C1}$ values as the population of the three rotamers *t*-A, g^+-B and g^--C. For example for **L-CCG-I**, see eqns. (5)–(7).

$$^3J_{H2H3} = P_A J_t + P_B J_g + P_C J_g \quad (5)$$

$$^3J_{H3C1} = P_A J_g + P_B J_t + P_C J_g \quad (6)$$

$$P_A + P_B + P_C = 1 \quad (7)$$

In what follows, we will calculate the theoretical values of the conformationally informative coupling constants, J_g and J_t of torsion angles computed by MD for **L-CCG-I** and for **L-CCG-IV**, using Karplus-type equations (Table 2). For **L-CCG-I**, the coupling constants measured from H(3) and simultaneously from H(2) protons ($^3J_{H2H3}$, $^3J_{H3C1}$ and $^3J_{H2C4}$, $^3J_{H2C6}$) provide evidence for the identification of its major *trans* 'A' χ_1 rotamer (75%). The differences with the calculated coupling constants of the 'A' χ_1 conformation were larger than the experimental error (0.3 Hz) and were interpreted as a slight contribution of the *gauche* conformations which are approximately evaluated as 'B' (15%) and 'C' (10%). At the same time, the experimental $^3J_{H2H3}$, $^3J_{H3C1}$ and $^3J_{H2C4}$, $^3J_{H2C6}$ values (Table 2) for **L-CCG-IV**, should confirm the major *gauche* 'B' χ_1 rotamer (45%) and should include participation of conformations 'A' (35%) and 'C' (20%).

It is thus concluded, from NMR data, that **L-CCG-I** exists in solution as two major rotamers *t*-A and *eclipsed*-a* and **L-CCG-IV** as two major rotamers g^+-B and *eclipsed*-c*. The preferred conformations, *t*-A and g^+-B respectively, are sterically favoured with the *trans* H(2)–H(3) conformations (γ-CO_2^- and side-chain *trans*). These conformers are very likely stabilized by the minimum of interactions between the cyclopropane ring and the α-amino and α-carboxylate groups [Figs. 3(*a*) and 4(*a*)]. Other minor conformation(s) could also participate in solution, such as g^+-B and g^--C for **L-CCG-I** or *t*-A and g^--C for **L-CCG-IV**.

Molecular modelling

The aims of the molecular modelling are as follows. (*i*) To select a set of conformations to be considered in the conformational analysis of NMR data. The computed torsion angles then form a basis for determination of the experimental conformer populations *via* Karplus equations. (*ii*) To evaluate the theoretical conformer populations and compare them with the experimental ones. This can be achieved *via* Maxwell–Boltzmann statistics or by molecular dynamics (MD) calculations. We will show below that only MD simulations give good results.

Whatever the aim, we have to choose how to describe the intra- and inter-molecular interactions. A good procedure for choosing the appropriate force field to identify the experimentally determined conformation as the lowest energy structure is to fit the parameters of the interaction function to results (potential or field) of *ab initio* quantum calculations on a small molecular cluster. The alternative is to fit the force field parameters on experimental data such as, in our case, NMR data. We have chosen this second way and in order to develop an adequate molecular model of the two analogues, we have tested the ability of two force fields, CVFF[38] and TRIPOS[39] (as implemented in BIOSYM and SYBYL programs, respectively), to reproduce the NMR experimental data.

The cyclopropane molecule is less stable than molecules with larger rings, and the difference in energy is referred to as angle strain. Since the three carbon atoms of a cyclopropane ring are required by symmetry to be at the vertices of an equilateral triangle, this arrangement represents a serious distortion of the normal tetrahedral bond angle and engenders unique chemical and physical properties. To develop a valence bond model of the bonding in cyclopropane, it is assumed that the carbon atoms will adopt the hybridization that produces the most stable bonding arrangement. Consequently, the carbon atom orbitals must have increased s character. The change in hybridization is associated with a change in electronegativity. The greater the s character, the greater is the electronegativity of a particular carbon atom. As a result, strained carbon atoms are more electronegative than unstrained ones[40] hence the need to calculate the charges with caution.

For this reason, the different experiments of molecular modelling were undertaken with different calculated values of atomic charges obtained for the cyclopropane (Table S3). (*i*) The charges Q1 in the residue library, implemented in the CVFF force field, are results of fits to crystal properties. They were derived by empirical fitting, that is adjusting the potential parameters and charges until they can reproduce the crystal structure.[41,42] As we will see below, they lead to a poor agreement with experiments. Two other sources of atomic charges were used, coming from *ab initio* quantum calculations at the RHF level (GAUSSIAN94). These charges Q2 (STO-3G//STO-3G)[43] and Q3 (6-31G//6-31G)[44] are introduced in the CVFF force field. (*ii*) The charges are computed by semi-empirical quantum methods AM1[45] (Q4), Del Re[46] (Q5) and Pullman[47] (Q6) and introduced in the TRIPOS force field. The optimized geometries and the corresponding energies are given in Tables 3 and 4.

Particular attention had to be given to the modelling of electrostatic interactions which are calculated in the force field by a coulombic expression. A widely used method to mimic the solvent screening effect is to use a distance-dependent relative permittivity $\varepsilon = r$, leading to an r^2 dependence of the coulombic

Table 3 Energies (kcal mol^{-1}) and Boltzmann probabilities (%) of the three lowest energy conformations for the **L-CCG-I** isomer. Molecular mechanic experiments were undertaken with different values in the force field equations of calculated atomic charges (for the cyclopropane) and relative permittivities ε.

	CVFF										TRIPOS			
	Protocol[f]										Protocol			
	1		2		3		4		5		1		2	
Conformer	E	%	E	%	E	%	E	%	E	%	E	%	E	%
Q1 (CVFF)[a]											Q4 (AM1)[c]			
A	101.3	100	108.3	100	−554.1	0	104.0	100	109.4	100	95.2	100	100.5	98.5
B	107.9	0	113.5	0	−648.1	100	108.0	0	113.4	0	100.1	0	103.2	1.0
C	108.6	0	114.6	0	−538.0	0	108.4	0	113.8	0	100.0	0	103.7	0.5
Q2 (STO-3G//STO-3G)[b]											Q5 (Del Re)[d]			
A	116.2	100	113.6	100	−402.1	100	112.5	100	112.3	100	79.7	100	94.1	98.5
B	120.2	0	117.5	0	−127.3	0	126.4	0	130.6	0	84.2	0	96.7	1.3
C	141.0	0	132.0	0	−150.0	0	132.4	0	132.4	0	84.8	0	97.7	0.2
Q3 (631-G//631-G)[b]											Q6 (Pullman)[e]			
A	131.5	100	121.7	100	−414.8	100	130.9	100	121.3	100	77.7	100	93.3	98.5
B	150.2	0	139.8	0	−208.4	0	161.4	0	151.8	0	82.0	0	95.8	1.5
C	143.8	0	136.7	0	−147.5	0	155.4	0	145.8	0	83.2	0	97.1	0

[a] The charges Q1 in the residue library, implemented in the CVFF force field are derived by empirical fitting,[51,52] *i.e.* adjusting the potential parameters and charges until they can reproduce the crystal structure. [b] The charges Q2 (STO-3G//STO-3G)[53] and Q3 (6-31G//6-31G)[54] are introduced in the CVFF force field coming from *ab initio* quantum calculations at the RHF level (GAUSSIAN94). [c] The charges Q4 (AM1)[55] are calculated by a semi-empirical molecular orbital method AM1 implanted in the MOPAC package. [d] The charges Q5 (Del Re)[56] are calculated by a quantum chemical method using the concept of localized bond orbitals. [e] The charges Q6 (Pullman)[57] are the sum of the charges calculated by two methods: the Hückel method to calculate the π component of the atomic charge and the Del Re method to calculate the σ component. [f] Protocols: (1) with $\varepsilon = 5$ at pH 7; (2) with $\varepsilon = 4r$ at pH 7; (3) in a water box (the energy obtained are those of 'molecule + 48 H_2O' systems); (4) with $\varepsilon = 5$ at pH 3; (5) with $\varepsilon = 4r$ at pH 3.

Table 4 Energies (kcal mol^{-1}) and Boltzmann probabilities (%) of the three lowest energy conformations for the **L-CCG-IV** isomer. Molecular mechanic experiments were undertaken with different values in the force field equations of calculated atomic charges (for the cyclopropane) and relative permittivities ε.

	CVFF										TRIPOS			
	Protocol[f]										Protocol			
	1		2		3		4		5		1		2	
Conformer	E	%	E	%	E	%	E	%	E	%	E	%	E	%
Q1 (CVFF)[a]											Q4 (AM1)[c]			
A	103.2	100	111.2	42	−533.3	0	108.9	0	114.5	100	93.8	100	99.7	73.5
B	106.0	0	111.0	58	−522.1	0	104.2	100	109.7	0	101.3	0	103.1	0
C	190.7	0	114.8	0	−537.8	100	109.3	0	114.4	0	96.6	0	100.3	26.5
Q2 (STO-3G//STO-3G)[b]											Q5 (Del Re)[d]			
A	125.0	0	122.1	0	−160.2	0	122.5	0	122.4	0	77.8	100	92.6	99.5
B	118.5	100	115.0	100	−432.1	100	112.2	100	112.4	100	85.6	0	97.3	0.5
C	131.7	0	126.2	0	−163.2	0	129.7	0	129.4	0	83.9	0	95.9	0
Q3 (631-G//631-G)[b]											Q6 (Pullman)[e]			
A	64.7	0	101.6	0	−565.3	0	87.4	0	108.0	0	75.2	100	108.0	0
B	61.3	100	97.1	100	−953.6	100	78.4	100	99.7	100	83.6	0	99.7	98.0
C	74.4	0	112.6	0	−674.0	0	80.4	0	102.1	0	82.1	0	102.1	2.0

[a,b,c,d,e] See notes in Table 3. [f] Protocols: (1) with $\varepsilon = 5$ at pH 7; (2) with $\varepsilon = 4r$ at pH 7; (3) in a water box (the energy obtained are those of 'molecule + 48 H_2O' systems); (4) with $\varepsilon = 5$ at pH 3; (5) with $\varepsilon = 4r$ at pH 3.

energy.[48] In previous studies,[15] to model implicitly the solvent effect, we adjusted the relative permittivity to a value, between 1 and 78 ($\varepsilon = 5$ and $4r$), corresponding to the interactions in aqueous solution. However, it is better to mimic the solvent with explicit modelling of water. So, we constructed solvation boxes around the charged end groups of the molecules containing several water molecules by using periodic boundary conditions.[49]

In addition to getting the best agreement between theoretical (MD) and experimental (NMR) data, the purpose of this work is also to give some insight into the water exchange on the three ions. Simulations were carried out on systems **L-CCG-I** and **L-CCG-IV** containing one positive ammonium ion and two negative carboxylate ions and a reasonable number of water molecules (48). Because of the presence of the cyclopropyl group on the same carbon that bears the ammonium and carboxylate groups, the hydration of the molecule is mainly governed by electrostatic and steric factors to represent the water–water intermolecular interactions, the ion–water interaction and the ligand–field effects.

The experimental populations change with pH. Of course, the molecular modelling can only implicitly take the pH into

Table 5 Results of the MD simulations using different protocols[a] and starting from the three conformations of the two isomers: **L-CCG-I** and **L-CCG-IV** at different pH values. The experiments are undertaken with the CVFF force field and the charges Q1 (CVFF),[b] Q2 (STO-3G//STO-3G)[c] and Q3 (6-31G//6-31G).[c]

		L-CCG-I																			
		Q1								Q2						Q3					
		Protocol[a]								Protocol						Protocol					
Conformer	NMR	1	2	3	4	5	6	7	8	3	4	5	6	7	8	3	4	5	6	7	8
A	75	100	100	100	100	96	100	4	1	100	100	92	75	65	35	100	100	95	100	7	36
B	20	0	0	0	0	0	0	44	49	0	0	0	5	30	40	0	0	4	0	92	61
C	5	0	0	0	0	4	0	52	51	0	0	2	20	5	15	0	0	1	0	1	12
		L-CCG-IV																			
		Q1								Q2						Q3					
		Protocol[a]								Protocol						Protocol					
Conformer	NMR	1	2	3	4	5	6	7	8	3	4	5	6	7	8	3	4	5	6	7	8
A	35	95	67	98	70	7	0	0	0	34	35	0	0	35	0	99	100	0	0	10	0
B	40	5	33	2	30	93	100	100	100	66	65	100	100	35	100	0	0	85	65	55	65
C	25	0	0	0	0	0	0	0	0	0	0	0	0	30	0	1	0	15	35	35	35

[a] Protocols: (1) 50 ps MD run at 300–600 K with $\varepsilon = 4r$ at pH 7; (2) 200 ps MD run at 300 K with $\varepsilon = 4r$ at pH 7; (3) 50 ps MD run at 300–600 K with $\varepsilon = 5$ at pH 7; (4) 200 ps MD run at 300 K with $\varepsilon = 5$ at pH 7; (5) 50 ps MD run at 300–600 K with $\varepsilon = 5$ at pH 3; (6) 200 ps MD run at 300 K with $\varepsilon = 5$ at pH 3; (7) 50 ps MD run at 300–600 K in a water box; (8) 200 ps MD run at 300 K in a water box. [b] The charges Q1[52,53] implemented in the CVFF force field are derived by empirical fitting to crystal properties. [c] The charges Q2 (STO-3G//STO-3G)[54] and Q3 (6-31G//6-31G)[55] are introduced in the CVFF force field coming from *ab initio* quantum calculations at the RHF level (GAUSSIAN94).

account working on the protonated or non-protonated species favoured at pH 3 (α-CO_2H, γ-CO_2^- and α-NH_3^+), pH 7 (α-CO_2^-, γ-CO_2^- and α-NH_3^+) and pH 10 (α-CO_2^-, γ-CO_2^- and α-NH_2).

Molecular mechanics. The first step of modelling consists of minimizing the structure previously constructed, to find a local energy minimum. A protocol was conceived that would rapidly give results in conformational studies, avoiding the introduction of explicit water molecules ($\varepsilon = 5$ and $4r$). The results are summarized in Tables 3 and 4.

The relative population of the ith conformational state, P_i with energy E_i, is dictated by the Boltzmann distribution [eqn. (8)]. We have calculated the population of different con-

$$P_i = \exp(-E_i/kT)/\Sigma \exp(-E_i/kT) \qquad (8)$$

formations using Maxwell-Boltzmann statistics.

Note that for **L-CCG-I**, most of the calculations lead to the good major rotamer ('A') in agreement with NMR results, but using Q1 charges implanted in CVFF force field and an explicit solvent description, rotamer 'B' is favoured (Table 3). For **L-CCG-IV**, the Boltzmann probabilities with the calculated charges (Q4 and Q5) and TRIPOS force field, lead to the major 'A' conformation while the results obtained with Q2 or Q3 calculated charges included in CVFF force field give the predominant NMR 'B' conformation (Table 4).

The ability of the CVFF force field to reproduce the experimental NMR-determined major conformations of **L-CCG-IV** (Bc*) suggests that the CVFF force field is an adequate tool for modelling these compounds.

The Boltzmann probabilities did not generate the approximate ratios of minimum-energy conformations available, respectively, for **L-CCG-I** and **L-CCG-IV** in aqueous solution. This result indicates that ranking the conformations according only to their potential energies could be misleading in certain cases. For these charged and flexible molecules, it is obvious that MD studies may have to be used to get more reasonable statistical participation of every structure to improve the NMR result.

Molecular dynamics. To simulate the molecular motions in solution, different protocols of molecular dynamics have been used. In MD calculations, the empirical force field methods are able to produce a collection of structures that span all the accessible conformational space of the molecule. In order to find suitable parameters (charge values, solvent and electrostatic terms, number of water molecules, times and temperature) for the simulation of these specific molecules, we varied them systematically and performed 132 simulations (Tables 5, S4 and S5).

We ran experiments starting from each one of the three possible conformations (obtained by combined incrementation of the side-chain bonds χ_1 and χ_2) of the two compounds (**L-CCG-I** and **L-CCG-IV**) to compare their energies and to determine their frequency in the interconversion. In addition, we carried out simulations starting from each one of the three conformers of **L-CCG-I** and **L-CCG-IV**, in various protonation states, with different values of ε and in an aqueous environment to get the best agreement between theoretical (MD) and experimental (NMR) data. These experiments lead to a statistical evaluation of the different conformations which contribute to the results obtained by NMR analysis. The ability of a force field to reproduce the experimental NMR-determined conformations suggests that no modification would be made in this appropriate force field for modelling the compounds.

The important electrostatic (the α-NH_3^+ and the γ-CO_2^- groups) and steric (cyclopropyl ring and intermediate eclipsed forms) contributions lead to a very good stabilization of some conformations and hinder an interconversion of the corresponding rotamers since the energetic barriers are too high. Consequently, in a first study, conformational analysis of these amino-acids began with the simple assumption of one dominating conformation, 't-A' in **L-CCG-I** and 'g^+-B' in **L-CCG-IV**. Most of the time, if MD experiments were performed from the three different starting structures, with implicitly taking account of the solvent ($\varepsilon = 5$ and $4r$) and with calculated charges (Q1–Q3) in the CVFF force field, they yielded the major rotamer. An ambiguity remains about the other low-energy conformers.

Each structure was further refined by putting the molecules (**L-CCG-I** and **L-CCG-IV**) in a solvent box of H_2O. As we will

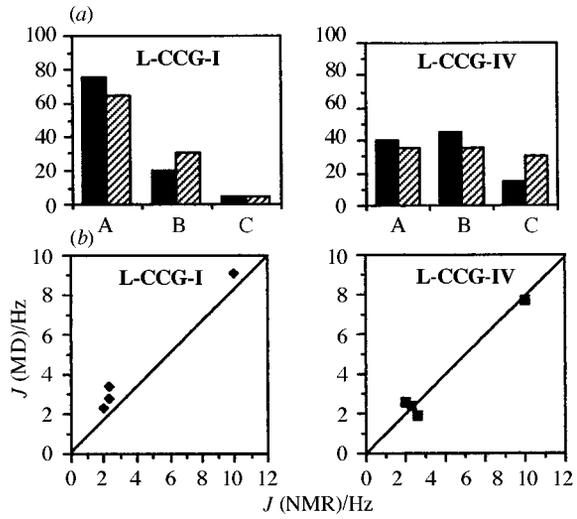

Fig. 5 (*a*) Correlation between the observed (NMR, ■) and calculated (MD, ▨) probabilities of the rotamers of the two isomers (**L-CCG-I** and **L-CCG-IV**), and (*b*) between the experimental (NMR) and calculated (MD) coupling constants using the populations calculated from the MD runs

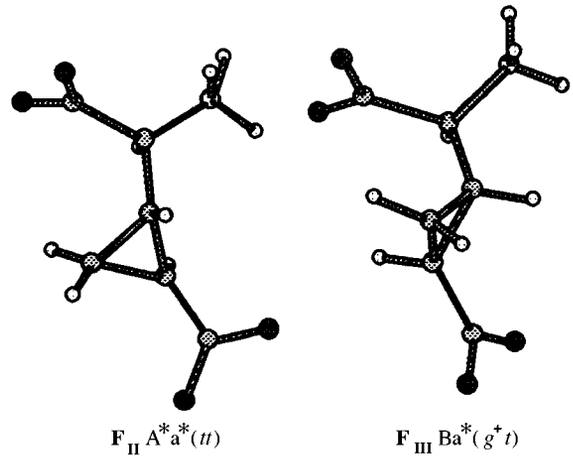

Fig. 6 Representation of the different conformational families $\mathbf{F_{II}}$, $\mathbf{F_{III}}$ corresponding to Aa* and Ba*, respectively

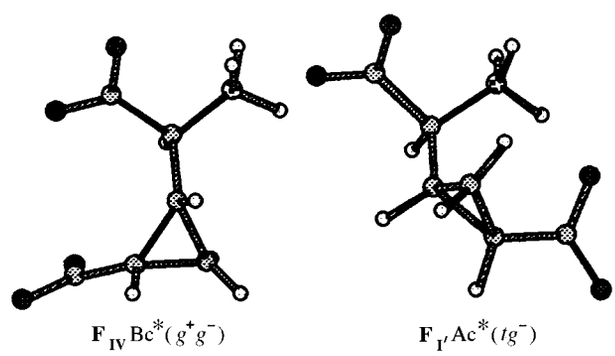

Fig. 7 Representation of the different conformational families $\mathbf{F_{IV}}$, $\mathbf{F_{I'}}$ corresponding to Bc* and Ac*, respectively

see below, the MD trajectories with hydration boxes and with Q2 (STO-3G) calculated charges in the CVFF force field were the most efficient in finding **L-CCG** conformations in agreement with NMR data.

L-CCG-I.—Protocols were carried out with the Q1 calculated charges in CVFF force field (Table S4 of the supplementary material) using different values of the relative permittivity ($\varepsilon = 5$ and $4r$). We observed that, whatever the protonation of the molecule is, the conformation 'A' was predominant or unique (100%). The differences observed between MD and NMR results have encouraged us to develop this study in a solvation box filled with water molecules in order to improve the composition of the solution. Different experiments were carried out but the minor NMR 'B' and 'C' conformations were generated in the same excess proportion (50%) (Table 5), whereas in the water box, with the CVFF force field and charges calculated by *ab initio* methods, STO-3G (Q2), the major conformation remains the 'A' one (~ 65%) while 'B' and 'C' conformations are now favoured (30% and 5%, respectively). This result is in good agreement with NMR data (MD/NMR): A (65/75), B (30/15) and C (5/10).

L-CCG-IV.—Most of the simulations lead to a unique or a very highly favoured conformation 'A' (and in some cases 'B'), whereas the experimental conformational mixture contains similar amounts of 'A', 'B' and 'C'. Here also, as for **L-CCG-I**, only the protocol with calculated charges Q2 (STO-3G) introduced in the CVFF force field and with explicit solvent description seems to be appropriate since good agreement is observed with the experimental NMR-determined populations. Indeed, from the various averaging resulting from the MD approach, the set 35% Ac* + 35% Bc* + 30% Cc* presented good agreement with the populations of rotamers obtained from NMR spectra (MD/NMR): A (35/35), B (35/45) and C (30/20) (Table 5, Fig. 5).

The fit between MD and the experimental data also indicates that the conformational space was well sampled.[50,51] The small difference is attributed to a slight variation of the minor conformers that affects the conformational averaging in solution.

The problem in using MD searching for ligand binding conformations, particularly if the ligands are ions or highly charged molecules is to not neglect protonation sites that will induce particular conformations. At pH 3 and 11, the electrostatic interactions are sufficiently reduced and conformations Aa* (**L-CCG-I**) and Bc* (**L-CCG-IV**) are sterically favoured (Tables 5 and S2). A quantitative interpretation of these data shows that besides a minor electrostatic term α-NH_3^+/γ-CO_2^-, a major steric repulsion exists in these analogues for such pairs of substituents as α-cyclopropyl/α-CO_2^-, α-cyclopropyl/α-NH_3^+ and α-CO_2^-/γ-CO_2^-.

Similarity analysis

Structural characteristics of the ligands. We have compared **L-CCG-I** (or **L-CCG-IV**) structures in terms of torsion angles χ_1 [α-CO–C(1)–C(2)–C(3)] and χ_2 [C(1)–C(2)–C(3)–γ-CO_2^-], corresponding to their relative flexibilities (Figs. 6 and 7 and Table 6). The molecular modelling calculations indicate that in the most stable conformations, torsion angles χ_1 are ~125–150° (**L-CCG-I**) and ~70–80° (**L-CCG-IV**) and χ_2 angles are ~135–150° (**L-CCG-I**) and ~ −10–0° (**L-CCG-IV**). This corresponds to the most populated conformations of **L-CCG-I** and **L-CCG-IV** determined by NMR analysis. The folded conformations g^+g^--Bc* and tg^--Ac* of **L-CCG-IV** and ~70% populated while the extended conformation *tt*-Aa* represents ~70% of the **L-CCG-I** solution.

Two groups are considered to have an electrostatic interaction if their distance is less than (or equal to) 4 Å. Rather than classify the conformational populations by combinations of χ_1 and χ_2, they have been collected according to the distances d_1 (α-NH–γ-CO_2^-) and d_2 (α-CO–γ-CO_2^-) in order to keep a limited number of families ($\mathbf{F_I}$–$\mathbf{F_{IV}}$) (Figs. 6 and 7 and Table 6). Two families were characterized by a d_1 distance shorter than d_2: d_1 min. ($d_1 \ll d_2$) and d_2 max. ($d_1 < d_2$). Conversely, two other families were characterized by a d_2 distance shorter than d_1: d_1 max. ($d_2 < d_1$) and d_2 min. ($d_2 \ll d_1$). Four other families ($\mathbf{F_{I'}}$–$\mathbf{F_{IV'}}$) with the same d_1 and d_2 distances will only differ in the sign of alkyl chain torsion angles χ_1 and χ_2.

Comparison between two specific metabotropic (group-II) agonists, L-CCG-I and (1*S*,3*R*)-*trans*-ACPD. The metabotropic

Table 6 Torsion angles (°) χ_1 [α-CO_2^-–C(2)–C(3)–C(4)] and χ_2 [$^+$NC(2)–C(3)–C(4)–γ-CO_2^-] and interatomic distances (Å) of specific agonists of metabotropic (*trans*-ACPD) and ionotropic NMDA (*cis*-ACDP) receptors. The maximal and minimal permissible distances: d_1 between the terminal carboxy carbon and the nitrogen (α-NH_3^+–γ-CO_2^-) and d_2 between the two carboxy carbon atoms (α-CO_2^-–γ-CO_2^-).

	d_1		d_2		χ_1		χ_2		
	Min.	Max.	Min.	Max.	Min.	Max.	Min.	Max.	Family[a]
trans-ACPD[b]	2.9	5.0	4.6	5.2	78.2	162.5	70.2	168.1	$\mathbf{F_I}$, $\mathbf{F_{II}}$, $\mathbf{F_{III}}$
L-CCG-I[c]									
Aa*	4.26		5.14		152.5		139.9		$\mathbf{F_I}$ $\mathbf{F_{II}}$
A*a	4.57		5.18		132.0		151.7		$\mathbf{F_{II}}$
A*a*	4.59		5.18		125.1		146.0		$\mathbf{F_{II}}$
Ba*	4.92		4.8		55.8		136.8		$\mathbf{F_{III}}$
(1*S*,3*S*)-*cis*-ACPD[b]	4.6	5.0	3.1	5.1	78.2	162.5	197.9 (−17.9)	283.5 (−76.5)	$\mathbf{F_{II}}$,$\mathbf{F_{III}}$,$\mathbf{F_{IV}}$
L-CCG-IV[c]									
Bc*	4.84		3.87		79.5		1.9		$\mathbf{F_{III}}$ $\mathbf{F_{IV}}$
B*c*	4.95		3.72		71.0		−8.3		$\mathbf{F_{IV}}$

[a] The different families ($\mathbf{F_I}$–$\mathbf{F_{IV}}$) are defined by the distances d_1 (α-NH–γ-CO_2^-) and d_2 (α-CO–γ-CO_2^-). Two families were characterized by a d_1 distance shorter than d_2: $\mathbf{F_I}$ (d_1 min, $d_1 \ll d_2$) and $\mathbf{F_{II}}$ (d_2 max, $d_1 < d_2$). Conversely, two other families were characterized by a d_2 distance shorter than d_1: $\mathbf{F_{III}}$ (d_1 max, $d_2 < d_1$) and $\mathbf{F_{IV}}$ (d_2 min, $d_2 \ll d_1$). Four other families ($\mathbf{F_{I'}}$–$\mathbf{F_{IV'}}$) with the same d_1, d_2 distances will only differ in the sign of alkyl chain torsion angles χ_1, χ_2. The families $\mathbf{F_I}$–$\mathbf{F_{IV}}$ correspond to the different conformations, Aa* ($\mathbf{F_{II}}$), Ba* ($\mathbf{F_{III}}$) and Bc* ($\mathbf{F_{IV}}$) while the families $\mathbf{F_{I'}}$–$\mathbf{F_{IV'}}$ correspond to the different conformations Ac*, Cc* ($\mathbf{F_{I'}}$) and Ca* ($\mathbf{F_{III'}}$). [b] The two distances (d_1 and d_2) and the torsion angles χ_1 and χ_2 are obtained for the different envelope forms for the cyclopentane, (1*S*,3*R*)-*trans*-ACPD and (1*S*,3*S*)-*cis*-ACPD. The analogue (1*S*,3*R*)-*trans*-ACPD belongs to the conformational families $\mathbf{F_I}$ [χ_1 (120–165: A, A*); χ_2 (75–105: b, b*); d_1 (2.87–3.64); d_2 (4.55–5.01)], $\mathbf{F_{II}}$ [χ_1 (90–145: B*, A*); χ_2 (120–150: a*); d_1 (4.15–4.58); d_2 (4.76–5.22)] and $\mathbf{F_{III}}$ [χ_1 (78–98: B*); χ_2 (140–168: a*, a); d_1 (4.76–4.96); d_2 (4.72–4.83)]. The *cis*-ACPD belongs to the conformational classes: $\mathbf{F_{II}}$ [χ_1 (122–163: A, A*); χ_2 (−142)–(−162): a, a*; d_1 (4.60–4.94); d_2 (4.63–5.06)] and $\mathbf{F_{IV}}$ [χ (78–98: B, B*); χ_2 (−76)–(−108): c, c*; d_1 (4.56–4.90); d_2 (3.14–3.83)]. [c] We have represented the major conformations of **L-CCG-I** and **L-CCG-IV** isomers generated in solvation box during MD experiment (300 K jump to 600 K) with calculated charges Q2. Some conformations are in an 'eclipsed' form and represented by the symbol '*'.

glutamate receptors (mGluRs) are characterized by eight mGluRs[9,10] which are classified into three groups, of which group-II (mGluR2 and mGluR3) is activated by (1*S*,3*R*)-*trans*-ACPD and (2*S*,3*S*,4*S*)-**L-CCG-I**.[10,13,14]

The analogue **L-CCG-I** belongs mainly to the Aa* (and also to the A*a*) conformer (75%) at pH 7. This major conformer appears to be particularly stable and adopts an 'extended' conformation. The other minor conformations (Ba*, Ca*) are present to a lesser extent (15%) in the neutral solution. The study was made at different pH values (pH 3 and pH 11) to analyse the evolution of the different populations in the conformational equilibrium, but the conformational solution does not change appreciably as the pH changes.

The analogue (1*S*,3*R*)-*trans*-ACPD adopts multiple conformations (A, A*, B, B*, a, a*, b and b*) and in this agonist, the C(2)–C(3) and C(3)–C(4) rotors cannot adopt a g^--C and g^--c conformation, respectively. (1*S*,3*R*)-*trans*-ACPD can be considered an interesting tool for investigations on molecules such as **L-CCG-I** with approximately the same activity for the group-II.

We have compared the major conformations obtained for (1*S*,3*R*)-*trans*-ACPD with the two Aa* (and also A*a*) and Ba* conformations of **L-CCG-I** and we can observe that the Aa* and Ba* conformations fit well with the corresponding major conformations of the (1*S*,3*R*)-*trans*-ACPD (Table 6, Fig. 8).

The results obtained for (2*S*,3*S*,4*S*)-**L-CCG-I** and (1*S*,3*R*)-*trans*-ACPD agonists which both exhibited a mGluR2 (group-II) activity show that the *tt*-Aa or *tt*-Aa* conformation of glutamate embedded in these two cyclic metabotropic agonists is an important factor for the mGluR2 sub-type receptor.

Comparison between two specific ionotropic (NMDA) agonists, L-CCG-IV and (1*R*,3*R*)-*cis*-ACPD. The analogue **L-CCG-IV** belongs mainly to the Bc* (and also B*c*) conformer (45%) at pH 7. This major structure appears to be particularly stable and adopts a 'folded' conformation. The other minor conformations (Ac*, Cc*) are also present (55%) in the neutral solution.

It is well known that (1*R*,3*R*)-*cis*-ACPD was shown to be an effective agonist of NMDA receptors.[52,53] In a previous study,[16] conformational analysis has shown that *cis*-ACPD adopts multiple conformations (A, A*, B, B*, a, a*, c and c*) (Table 6). At physiological pH, both carboxy groups are found to be in an extended position (*tt*-Aa) to reduce the steric energy. At isoelectric pH when the 3-carboxylate group is protonated, *cis*-ACPD is represented by new privileged conformations (g^+g^--Bc) in which the 1-carboxylate group (α-CO_2^-) is stabilized by an electrostatic interaction with the folded 3-carboxy group (γ-CO_2H).

In a previous study, among five studied analogues, the (2*S*)-4-methyleneglutamic acid **4M** isomer presents a potent activity at the ionotropic glutamate receptors (NMDA).[54] For this compound, the conformational solution is represented by 60% of the g^+g^--Bc* conformation.

Since the **L-CCG-IV** isomer, the (1*S*,3*S*)-*cis*-ACPD and the **4M** isomer were found to preferentially activate NMDA receptors if we superimposed the three characteristic functional atoms α-N, α-C, γ-C of the conformations of the three NMDA agonists, we observed good agreement (Fig. 9). Our study has provided clear evidence that the conformation g^+g^--Bc (or B*c, Bc*) would be the most plausible conformation of glutamate required for binding to NMDA receptors.

Conclusions

The conformations of **L-CCG-I** and **L-CCG-IV** in aqueous solution have been elucidated by a conformational analysis using a combination of NMR experimental results, mechanics and dynamics calculations, and theoretical simulation of NMR spectra. It has been necessary to calculate the charge distri-

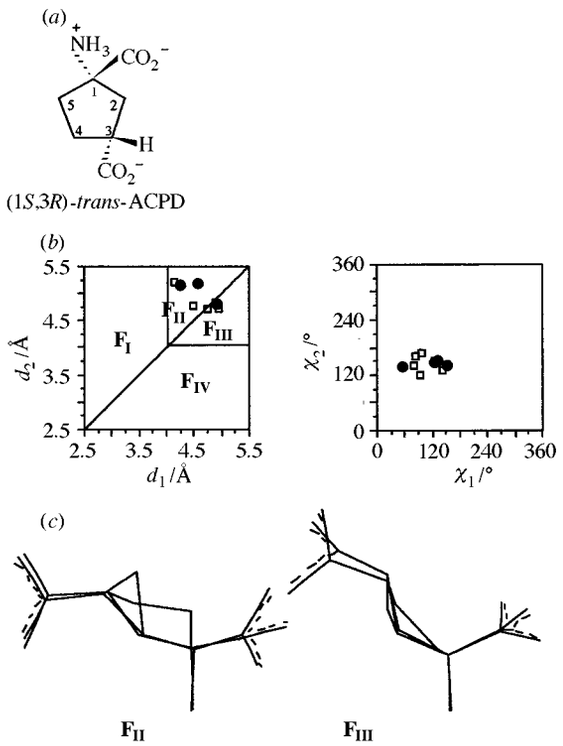

Fig. 8 (*a*) Structure of the (1*S*,3*R*)-*trans*-ACPD isomer in aqueous solution at pH 7. (*b*) Representation of the three conformational families $\mathbf{F_I}$, $\mathbf{F_{II}}$, $\mathbf{F_{III}}$ for the **L-CCG-I** isomer and the (1*S*,3*R*)-*trans*-ACPD according to their characteristic distances $d_{1(\alpha\text{-}NH_3^+\text{–}\gamma\text{-}CO_2^-)}$, $d_{2(\alpha\text{-}CO_2^-\text{–}\gamma\text{-}CO_2^-)}$ and their characteristic torsion angles χ_1 [α-CO_2^-–C(2)–C(3)–C(4)] and χ_2 [$^+$NC(2)–C(3)–C(4)–γ-CO_2^-]. The two distances (d_1 and d_2) and the torsion angles χ_1 and χ_2 are obtained for the different envelope forms for the cyclopentane, (1*S*,3*R*)-*trans*-ACPD. The analogue (1*S*,3*R*)-*trans*-ACPD belongs to the conformational families $\mathbf{F_I}$ [χ_1 (120–165: A, A*); χ_2 (75–105: b, b*); d_1 (2.87–3.64); d_2 (4.55–5.01)], $\mathbf{F_{II}}$ [χ_1 (90–145: B*, A*); χ_2 (120–150: a*); d_1 (4.15–4.58); d_2 (4.76–5.22)] and $\mathbf{F_{III}}$ [χ_1 (78–98: B*); χ_2 (140–168: a*, a); d_1 (4.76–4.96); d_2 (4.72–4.83)]. (*c*) Superimposition of the major structures of **L-CCG-I**, with the major structures of the (1*S*,3*R*)-*trans*-ACPD isomer belonging respectively to the family $\mathbf{F_{II}}$ (1*S*,3*R*)-*trans*-ACPD (^{5}E) and **L-CCG-I** Aa*, the family $\mathbf{F_{III}}$ (1*S*,3*R*)-*trans*-ACPD (E_2) and **L-CCG-I** Ba*. **L-CCG-I:** ●, *trans*-ACPD: □.

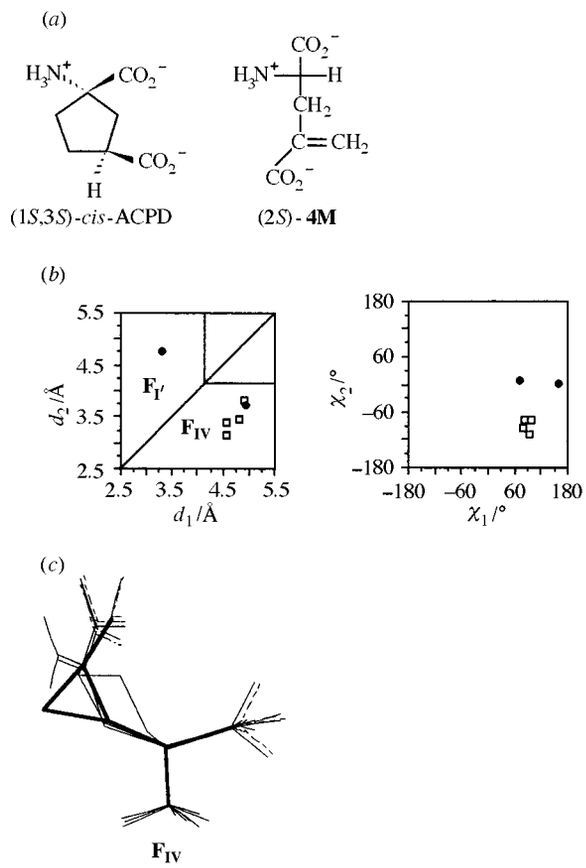

Fig. 9 (*a*) Structure of the (1*S*,3*S*)-*cis*-ACPD and **4M** isomer in aqueous solution at pH 7. (*b*) Representation of the three conformational families $\mathbf{F_{I'}}$, $\mathbf{F_{IV}}$ for the **L-CCG-IV** isomer and the (1*S*,3*S*)-*cis*-ACPD according to their characteristic distances $d_{1(\alpha\text{-}NH_3^+\text{–}\gamma\text{-}CO_2^-)}$, $d_{2(\alpha\text{-}CO_2^-\text{–}\gamma\text{-}CO_2^-)}$ and their characteristic torsion angles χ_1 [α-CO_2^-–C(2)–C(3)–C(4)] and χ_2 [$^+$NC(2)–C(3)–C(4)–γ-CO_2^-]. The two distances (d_1 and d_2) and the torsion angles χ_1 and χ_2 are obtained for the different envelope forms for the cyclopentane, (1*S*,3*S*)-*cis*-ACPD. The analogue *cis*-ACPD belongs to the conformational classes: $\mathbf{F_{II}}$ {χ_1 (122–163: A, A*); χ_2 [(−142)–(−162): a, a*]; d_1 (4.60–4.94); d_2 (4.63–5.06)} and $\mathbf{F_{IV}}$ {χ_1 (78–98: B, B*); χ_2 [(−76)–(−108): c, c*]; d_1 (4.56–4.90); d_2 (3.14–3.83)}. (*c*) Superimposition of the major structure Bc* of **L-CCG-IV** at neutral pH, with the major structures of the (1*S*,3*S*)-*cis*-ACPD (E_5) and **4M** (B*γ) belonging to the family $\mathbf{F_{IV}}$. **L-CCG-IV:** ●, *cis*-ACPD: □.

butions in the cyclopropane moiety by an *ab initio* quantum method and to include the results in the CVFF force field to fit molecular modelling and experimental NMR data.

This study shows clearly the structural position of the potentially active functional groups, α-NH_3^+, α-CO_2^- and γ-CO_2^- and the preferred '*t*-A' and 'g^+-B' conformations of the C(3) aminocarboxymethyl side-chain of **L-CCG-I** and **L-CCG-IV**, respectively.

The conformations may be grouped by the consideration of two backbone torsion angles, χ_1 [α-CO_2^-–C(2)–C(3)–C(4)] and χ_2 [$^+$NC(2)–C(3)–C(4)–γ-CO_2^-] and by consideration of the two characteristic distances between the potentially active functional groups, α-N^+ --- γ-CO_2^- (d_1) and α-CO_2^- --- γ-CO_2^- (d_2). The conformational preferences in solution of **L-CCG-I** and **L-CCG-IV** are discussed in the light of the physical features known for a specific metabotropic agonist (ACPD) and specific ionotropic agonists (NMDA), respectively. This aspect makes **L-CCG-I** and **L-CCG-IV** interesting tools for studies of conformation preferences of glutamate sub-type receptors. Thus, the binding conformations of the metabotropic receptors correspond to the conformation *t*-A, g^+-B and *t*-a, g^+-b relative to the C(2)–C(3) and C(3)–C(4) torsion angle, respectively.[55] In particular, the two *t*-A and g^+-b rotamers seem essential for the interaction at the mGluR1a receptor (group-I),[56] while the *t*-A and *t*-a rotamers seem to activate the mGluR2 (group-II) metabotropic receptor. For the ionotropic receptor, the *t*-A, g^+-B and *t*-a, g^--c rotamers represent the active forms with a selectivity for the two receptor sub-types as NMDA and KA receptors.[55] Whereas the *t*-A, g^--c activates KA receptors, the g^+-B, g^--c conformation activates NMDA receptors.

Experimental

NMR spectroscopy

All NMR spectra were recorded on a Bruker AMX-500 spectrometer equipped with an X32 computer. A sample of **L-CCG** (7.4 mg) was dissolved in D_2O (0.6 ml) to give a final concentration of 0.09 mol dm^{-3} for the different isomers. The pH (in fact pD = pH −0.4, uncorrected here) was adjusted by addition of DC1 or NaOD. At pH 7 the samples were dissolved in an aq. NaD_2PO_4–Na_2DPO_4 buffer, and it was possible to attain concentrations of 0.09 mol dm^{-3} for the ^{1}H and ^{13}C experiments. Degassed and sealed tubes were used for the nuclear Overhauser enhancement experiments.

The errors in the chemical shifts are 0.01 and 0.1 ppm for ^{1}H and ^{13}C, respectively. A crystal of 3-(trimethylsilyl)[2,2,3,3-$^2H_4$]propionic acid, sodium salt [$^2H_4$]TSP was used as internal reference for the proton shifts, and for the carbon a value of the absolute frequency was used. The coupling constants are given with a precision of 0.3 Hz. The spectrum simulation was carried out on a Macintosh II computer using the software NMR II.

Presaturation of the solvent was used for all the 1D and 2D ^{1}H experiments. Four spectra from 280 to 310 K were recorded.

The selective inept (INAPT)[25] spectrum recorded with 32 K data points with a selective excitation of the H(2) protons allowed us to differentiate the carbons.

The 2D ^{1}H,^{1}H COSY spectra were acquired by recording 128 FIDs of 512 points. The relaxation delay was set to 3.5 s. The spectral width was set to 2500 Hz for proton spectra and 31 250 Hz for carbon spectra. The 90° pulse was 5.7 μs, the relaxation delay 1 s, and each FID was acquired with 64 scans. 2D NMR spectra were recorded on a X32 computer using UXNMR software (Bruker). The data were zero-filled and the final size of the matrices was 2 × 1 K to 1024 and 512 points in f_2 and f_1 respectively, prior to double Fourier transformations with an unshifted sine-bell window function in both dimensions. Inverse correlation HMQC experiments[27] were recorded using a transfer delay ($1/2J_{C-H}$) of 3.33 ms.

The 2D J δ selective INEPT[32] experiment using polarization transfer from ^{1}H to ^{13}C gave long-range heteronuclear coupling constants ^3J (^{13}C–^{1}H). The selective excitation of a proton signal allows detection of a single doublet for the corresponding coupled carbon(s). At 500 MHz, selectivity was achieved by a DANTE-type pulse train generated by the decoupler channel. In this study, the ^3J (^{13}C–^{1}H) coupling constants were measured for the two rotors: the H(2) proton was excited for the H(2)–C(2)–C(3)–C(4). This experiment also allows us to analyse the 'A, B, C' rotamer populations. This experiment was carried out at 300 K with 256 scans of 4000 data points, 64 experiments, a spectral width of 220 ppm in f_2 and 0.125 ppm in f_1.

The 2D phase-sensitive ^{1}H NOESY experiment was performed in D_2O solution with $\tau_m = 0.5$ s and relaxation delay of 3.0 s. FIDs were acquired (256 scans) over 3086 Hz into a 2 K data block for 256 incremental values of the evolution time.

Computer simulations

The conformations of the compounds that were incorporated into the analysis were obtained using BIOSYM and SYBYL molecular modelling software on a Silicon Graphics workstation.

Energy minimization and MD simulations were performed using two force fields: the consistent valence force field (CVFF) from Dauber-Osguthorpe *et al.*[38] and the TRIPOS force field (SYBYL).[57] In the two force fields, some constraints may have to be applied to limit the system to stay within certain relevant and interesting regions. Indeed the cyclopropane is not fully tested in the libraries of BIOSYM and SYBYL softwares, thus to build the initial structures, we must take into account characteristic values of cyclopropane (internuclear angles and distances). It is interesting to note that distances of the cyclopropane bonds increase until breaking if molecular dynamics simulations are run without constraints.

Charges and atomic potentials come from six different sources (Table S3). The charges Q1 in the BIOSYM residue library are derived by empirical fitting, that is adjusting the potential parameters and charges until they can reproduce the crystal structure. Charges Q2 to Q6 are computed by molecular orbital treatments at the HF level. The first two are derived from *ab initio* calculations (GAUSSIAN94) using STO-3G (Q2) and 6-31G (Q3) basis tests. The other three are derived from semiempirical calculations. The charges Q4 come from the method AM1 implanted in the MOPAC package. The charges Q5 (Del Re) are calculated by a quantum chemical method using the concept of localized bond orbitals. The charges Q6 (Pullman) are the sum of the charges calculated by two methods: the Hückel method to calculate the π component of the atomic charge and the Del Re method to calculate the σ component.

The charge distributions resulting from a number of quantum calculations on the cyclopropyl **L-CCG-I** molecule are given in Table S3.

To mimic the solvent effect, the relative permittivity was set to be distance dependent, $\varepsilon = R_{ij}$ ($\varepsilon = 5$ and $4r$)[15] in the description of the coulombic interaction. Another protocol was used with explicit solvent molecules incorporated during the run. SYBYL software does not allow the user to select (and limit) the size of the solvent box. With BIOSYM software a best procedure was selected using a cube of volume 12 × 12 × 12 Å^3 containing 48 water molecules to allow periodic boundary conditions and a non-bonded cut-off distance of 11 Å. The relative permittivity was set to $\varepsilon = 1$. In these cases, the energy to be compared are those of 'molecule + $x$$H_2O$' systems in various situations.

The first step in the modelling consisted of minimizing the structure previously constructed, to find a local energy minimum on the potential energy hypersurface of the molecule. Calculations were performed according to several algorithms commonly used in molecular mechanics for choosing descent directions, namely steepest descent and conjugate gradient methods.

The second step of the conformational sampling procedure involved recording the MD trajectories (including the charge distributions Q1, Q2 and Q3 in the CVFF force field). By solving the equations of motion for a system of atoms, MD has an advantage in that it is not restricted to harmonic motion about a single minimum but allows molecules to cross energy barriers and explore other stable conformations. Molecular conformers were sampled during a 200 ps MD trajectory at 300 K (or 100 ps with 48 water molecules). A time step of 1 fs was used, and the system was equilibrated for 6 ps. A conformation was stored each picosecond so that 200 conformations (or 100 with 48 water molecules) were recorded by the end of the MD simulation. For a preliminary exploration of the conformational space, after energy minimization and an equilibration period of 6 ps, we performed a 50 ps MD run at 300 K with periodic temperature jumps to 600 K to supply the system with energy (to pass conformational barriers). The 50 ps trajectory is sampled every picosecond and the remaining structures are then minimized by molecular mechanics and stored. The final conformers found with lowest energies were then further minimized to a gradient less than 0.01 kcal mol^{-1} to obtain their energies at higher accuracy.

The sampling every picosecond was believed to be a sufficiently long time for an atom with significant movement and sufficiently short for a correct sampling of the conformational space. For an isolated molecule, the experiment takes about 15–30 min. For experiments in which the molecules are introduced into the solvation boxes, the CPU times are much longer (24 h or 48 h with BIOSYM software) according to the protocol.

All molecular conformations were compared using the analysis module of each software. Conformational similarities were evaluated by calculating the RMS of deviation between heavy atoms for each possible pair of the different structures. The results represent a group of structures whose small RMS deviations (<0.5 Å) suggested that they may belong to the same conformational family. Conformational representatives extracted from each family were compared for each compound, as well as between different ligands, using a superimposition procedure.

Acknowledgements

We thank Dr D. C. Sunter (TOCRIS Cookson Ltd, Bristol, UK) for providing **L-CCG-I** and **L-CCG-IV** samples. We acknowledge many suggestions from an exceptionally careful referee.

References

1 J. C. Watkins, P. Krogsgaard-Larsen and T. Honoré, *Trends Pharmacol. Sci.*, 1990, **11**, 25.
2 S. Nakanishi, *Science*, 1992, **258**, 597.

3 T. V. P. Bliss and G. L. Collingridge, *Nature* (*London*), 1993, **361**, 31.
4 D. T. Monoghan, R. J. Bridges and C. W. Cotman, *Ann. Rev. Pharmacol. Toxicol.*, 1989, **29**, 365.
5 R. H. Evans and J. C. Watkins, *Ann. Rev. Pharmacol. Toxicol.*, 1981, **21**, 165.
6 B. Sommer and P. H. Seeburg, *Trends Pharmacol. Sci.*, 1992, **13**, 291.
7 D. D. Schoepp and P. J. Conn, *Trends Pharmacol. Sci.*, 1993, **14**, 13.
8 J. P. Pin and R. Duvoisin, *Neuropharmacology*, 1995, **34**, 1.
9 T. Abe, H. Sugihara, H. Nawa, H. Shigemoto, N. Mizuno and S. Nakanishi, *J. Biol. Chem.*, 1992, **267**, 13 361.
10 Y. Tanabe, A. Nomura, M. Masu, R. Shigemoto, N. Mizuno and S. Nakanishi, *J. Neurosci.*, 1993, **13**, 1372.
11 J. Davies, R. H. Evans, A. A. Francis, A. W. Jones, D. A. S. Smith and J. C. Watkins, *Neurochem. Res.*, 1982, **7**, 1119.
12 R. Chamberlin and R. Bridges, *Conformationally constrained acidic amino acids as probes of Glutamate receptors and transporters*, Raven Press, New York, 1993.
13 Y. Ohfune and H. Shinozaki, *L-2-(Carboxycyclopropyl)glycines. Conformationally constrained L-glutamate analogues*, Raven Press, New York, 1993.
14 M. Ishida, T. Saitoh and H. Shinozaki, *Neurosci. Lett.*, 1993, **160**, 156.
15 N. Morelle, J. Gharbi-Benarous, F. Acher, G. Valle, M. Crisma, C. Toniolo, R. Azerad and J.-P. Girault, *J. Chem. Soc.*, *Perkin Trans. 2*, 1993, 525.
16 V. Larue, J. Gharbi-Benarous, F. Acher, G. Valle, M. Crisma, C. Toniolo, R. Azerad and J.-P. Girault, *J. Chem. Soc.*, *Perkin Trans. 2*, 1995, 1111.
17 K. Shimamoto, M. Ishida, H. Shinozaki and Y. Ohfune, *J. Org. Chem.*, 1991, **56**, 4167.
18 G. Costantino, B. Natalini, R. Pellicciari, F. Moroni and G. Lombardi, *Bioorg. Med. Chem.*, 1993, **4**, 259.
19 E. L. Eliel, N. L. Allinger, S. J. Angyal and G. A. Morrison, *Conformational Analysis*, Wiley, New York, 1965.
20 O. Bastiansen and A. de Meijere, *Acta Chem. Scand.*, 1966, **20**, 516.
21 O. Bastiansen and A. de Meijere, *Acta Chem. Scand.*, 1966, **78**, 142.
22 H. Günther and D. Wendisch, *Angew. Chem.*, 1966, **78**, 266.
23 W. Lüttke and A. de Meijere, *Angew. Chem.*, 1966, **78**, 544.
24 M. R. Bendall and D. T. Pegg, *J. Magn. Reson.*, 1983, **53**, 272.
25 A. Bax, *J. Magn. Reson.*, 1984, **57**, 314.
26 L. J. Lin and G. A. Cordell, *J. Chem. Soc.*, *Chem. Commun.*, 1986, 377.
27 R. E. Hurd and B. K. John, *J. Magn. Reson.*, 1991, **91**, 648.
28 H. Kessler, C. Griesinger and K. Wagner, *J. Am. Chem. Soc.*, 1987, **109**, 6927.
29 O. Jardetzky, *Biochim. Biophys. Acta*, 1980, **621**, 227.
30 O. Jardetzky and G. C. K. Roberts, *NMR in molecular biology*, Academic Press, New York, 1981.
31 G. C. K. Roberts and O. Jardetzky, *Adv. Protein Chem.*, 1970, **24**, 447.
32 P. Ladam, J. Gharbi-Benarous, M. Pioto, M. Delaforge and J.-P. Girault, *Magn. Reson. Chem.*, 1994, **32**, 1.
33 A. De Marco, M. Llinás and K. Wüthrich, *Biopolymers*, 1978, **17**, 637.
34 H. Günther, H. Klose and D. Cremer, *Chem. Ber.*, 1971, **104**, 3884.
35 C. A. G. Haasnoot, F. A. A. M. De Leeuw and C. Altona, *Tetrahedron*, 1980, **36**, 2783.
36 I. Tvaroska, M. Hricovini and E. Petrakova, *Carbohydr. Res.*, 1989, **189**, 359.
37 H. Günther, *NMR Spectroscopy*, Wiley, New York, 1994.
38 P. Dauber-Osguthorpe, V. A. Roberts, D. J. Osguthorpe, J. Wolff, M. Genest and A. T. Hagler, *Proteins: Struct.*, *Funct. and Genet.*, 1988, **4**, 31.
39 M. Clark, R. D. Cramer and N. Van Opdenbosh, *J. Comput. Chem.*, 1989, **10**, 982.
40 K. B. Wiberg, R. F. W. Bader and C. D. H. Lau, *J. Am. Chem. Soc.*, 1987, **109**, 1001.
41 A. T. Hagler, S. Lifson and P. Dauber, *J. Am. Chem. Soc.*, 1979, **101**, 5122.
42 A. T. Hagler, S. Lifson and P. Dauber, *J. Am. Chem. Soc.*, 1979, **101**, 5131.
43 W. J. Hehre, R. F. Stewart and J. A. Pople, *J. Chem. Phys.*, 1971, **51**, 2657.
44 W. J. Hehre, R. Ditchfield and J. A. Pople, *J. Chem. Phys.*, 1972, **56**, 2257.
45 J. J. Stewart, *J. Comp.-Aided Mol. Des.*, 1990, **4**, 1.
46 G. Del Re, *J. Am. Chem. Soc.*, 1958, 4031.
47 H. Berthod and A. Pullman, *J. Chem. Phys.*, 1965, **62**, 942.
48 S. K. Burt, D. Mackay and A. T. Nagler, *Computer-Aided Drug Design*, Marcel Dekker and Basel, New York, 1989.
49 W. F. van Gunsteren and H. J. C. Berendsen, *Angew. Chem.*, *Int. Ed. Engl.*, 1990, **29**, 992.
50 H. Kessler, C. Griesinger, J. Lautz, A. Müller, W. F. van Gunsteren and H. J. C. Berendsen, *J. Am. Chem. Soc.*, 1988, **110**, 3393.
51 P. H. Hünenberger, A. E. Mark and W. F. van Gunsteren, *J. Mol. Biol.*, 1995, **252**, 492.
52 K. Curry, M. J. Peet, D. S. K. Magnuson and H. McLennan, *J. Med Chem.*, 1988, **31**, 864.
53 K. Curry, *Can. J. Physiol. Pharmacol.*, 1991, **69**, 1076.
54 Z. Q. Gu, D. Hesson, J. C. Pelletier and M. L. Meccechini, *J. Med. Chem.*, 1995, **38**, 2518.
55 N. Todeschi, J. Gharbi-Benarous, F. Acher, V. Larue, J. P. Pin, J. Bockaert, R. Azerad and J.-P. Girault, *Bioog. Med. Chem.*, 1997, **5**, 335.
56 N. Todeschi, J. Gharbi-Benarous, F. Acher, R. Azerad and J.-P. Girault, *J. Chem. Soc.*, *Perkin Trans. 2*, 1996, 1337.
57 SYBYL, TRIPOS, St. Louis, MO, 1992.

Paper 7/03833J
Received 2nd *June* 1997
Accepted 25th *July* 1997